



Cite this: *Soft Matter*, 2018, 14, 8604

Received 13th July 2018,
Accepted 7th October 2018

DOI: 10.1039/c8sm01443d

rsc.li/soft-matter-journal

Segmental and secondary dynamics of nanoparticle-grafted oligomers

Adam P. Holt ^{ab} and C. M. Roland ^{a*}

The local segmental and secondary dynamics of tetramethylene oxide oligomer grafted to silica nanoparticles (NPs) were investigated as a function of grafting density and molecular weight. Grafting slows the segmental (α) dynamics, but gives rise to faster secondary (β) motions. Interestingly, the magnitude of these effects decreases with the extent of grafting (*i.e.*, surface coverage), as well as with oligomer molecular weight. The disparity in dynamical effects reflects the decoupling of the segmental and more local β dynamics, the former is associated with stronger dynamic correlations that extend over a greater spatial range. This results in greater sensitivity to interactions, including tethering of the chains to the NP surface.

Introduction

A principle objective of developing structured polymers (block copolymers, thin film laminates, nanocomposites, *etc.*) is control of their physical properties by tuning specific variables on the nanoscale.^{1,2} An obvious focus of such endeavors is modification of the interfacial regions of these materials, either structurally or dynamically.^{3–8} The interfacial dynamics can be affected on different timescales, and consequently exhibit diverse changes in physical properties. For example, the chain dynamics which governs the elasticity, diffusion, and rheological properties has been shown to be strongly affected by grafting (*e.g.*, tethering) of the chains to the surface of flat substrates or nanoparticles.^{9–13} Conventionally, the thermodynamic and mechanical properties of polymers are altered by controlling the segmental dynamics *via* plasticizers (or anti-plasticizers) and by chemical crosslinking;¹⁴ however, with adequate dispersion, chemisorption to nanoparticles also can produce similar effects.^{15–21} In addition to the chain dynamics, an often overlooked motion in polymers is the localized secondary processes measured below the glass transition temperature, T_g . Properties of these β relaxations correlate with some macroscopic mechanical properties of glassy polymers.^{22–25}

It has become apparent that the molecular weight, M_w , of interfacial polymer chains is a key factor determining the magnitude of confinement effects,^{26–31} which can be manifested on time scales both faster and slower than the segmental dynamics.^{32–36} In this work we investigate the local segmental and secondary dynamics of oligomeric polyamines grafted to

nanoparticles. To understand how the interphase alters the dynamics, experimental variables included both grafting density and oligomer M_w . Attaching chains to nanoparticles affects their dynamics on more than one time scale. Above T_g , the segmental dynamics usually become slower, with the magnitude of the effect increasing with decreasing molecular weight or decreasing grafting density. In contrast, herein we find that the secondary dynamics become faster, to a greater degree for lower M_w or lower grafting density.

Methods and materials

The spherical silica nanoparticles (radius $r_{np} = 7 \pm 1$ nm) from Nissan Chemicals were received as a dispersion in methyl ethyl ketone (MEK). The concentration of surface hydroxyl groups was ~ 4000 per particle, corresponding to ~ 7 per nm^2 , as determined by thermogravimetric analysis (TGA; TA Instruments Q500) and consistent with the manufacturer's specification. These were reacted with polycarbodiimide-modified diphenylmethane diisocyanate (Isonate 143L, Dow Chemical), followed by reaction with poly(tetramethylene oxide-*di-p*-aminobenzoate) (Air Products Versalink P650, P1000, P2000, corresponding to $M_w = 0.65, 1.25,$ and 2.25 kg mol^{-1} , respectively) at a 1 : 1 molar ratio to form the oligomer grafted nanoparticles (OGN) (Fig. 1). These reactions were carried out in the MEK solution (a good solvent for the oligomer). The radius of gyration of the (ungrafted) oligomers vary with molecular weight in the range 1 to 3 nm.³⁷ Grafting densities, σ_g , were determined by TGA and assume complete reaction of the isocyanate with the hydroxyl groups. This is corroborated by FTIR measurements indicating the disappearance of the isocyanate absorption band in the infrared spectrum.³⁸ A minute amount of free oligomer may be present, but is considered unlikely.

^a Chemistry Division, Naval Research Laboratory, Code 6105, Washington, DC, 20375-5342, USA. E-mail: mike.roland@nrl.navy.mil

^b American Society of Engineering Education, Washington, DC, 20036, USA

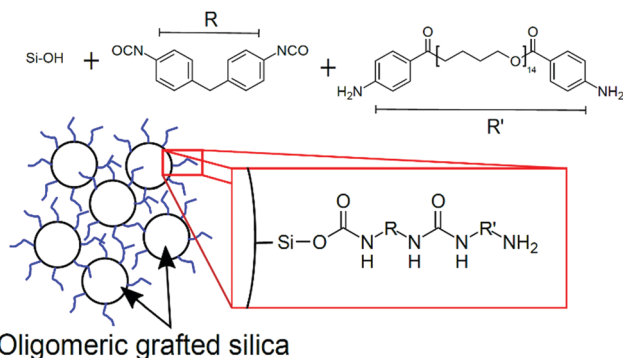


Fig. 1 Diisocyanate (R), oligomeric diamine (R'), and the resulting grafted silica nanoparticles.

Table 1 Physical characteristics of OGN ($M_w = 1.25 \text{ kg mol}^{-1}$)

σ_g (chains per nm^2)	$\ell = R_H - R_{\text{NP}}$ (nm)
0.59	3.75
0.20	0.94
0.03	0.35

The hydrodynamic radii, R_H , of the functionalized particles were measured in dilute solutions of MEK using dynamic light scattering at room temperature (DynaPro Nanostar, with $\lambda = 658 \text{ nm}$ and $\theta = 90^\circ$). Mass densities were obtained by the buoyance method (Archimedes principle), with DOW Corning 200 oil as the displacement liquid for the solid samples, and helium as the displacement gas for the powdered samples. The typical uncertainty in the density measurement was 1%. Representative data, including the size of the grafted polymer layer, ℓ , are listed in Table 1 for the intermediate M_w grafted chains. Note that less than 10% of the surface hydroxyl groups are reacted, so that the effective grafted region at the interface is less than half the size of the unbound polymer chain.

Conventional and temperature-modulated differential scanning calorimetry (TMDSC) was carried out with a TA Instruments Q100. Prior to measurements, samples were degassed overnight at 50°C *in vacuo*. The ungrafted higher molecular weight (1.25 and 2.25 kg mol^{-1}) oligomers crystallized at $10^\circ \text{C min}^{-1}$ or slower cooling; the lowest M_w oligomer showed no indication of crystallization. Grafting to the silica suppressed crystallization for the $M_w = 1.25 \text{ kg mol}^{-1}$ sample at all grafting densities, but had no effect on crystallization of the highest molecular weight oligomer. For the TMDSC measurements, the samples were equilibrated at 100°C , quenched to -150°C , and then heated at $2^\circ \text{C min}^{-1}$ to 100°C with a modulation amplitude of $0.32^\circ \text{C min}^{-1}$.

Dielectric spectroscopy (BDS) employed a Novocontrol Alpha-A analyzer. Sample temperature was controlled with a helium cryostat (Cryo Industries, Model 1899-350). Additional high frequency measurements were obtained with a Hewlett Packard 4291A RF impedance analyzer, 16453A test station, and 16092A head. For these measurements, the temperature profile was identical to that used in the calorimetry experiments. Crystallization of the neat polymer ($M_w = 1.25 \text{ kg mol}^{-1}$) was avoided by quenching with liquid nitrogen below T_g , with data subsequently obtained isothermally on heating.

Results

Effect of grafting density

The mass densities of the OGN are listed in Table 2 and plotted in Fig. 2 (normalized by the density of the neat oligomer). At constant M_w , there is a monotonic increase in the relative density with decreasing grafting density (since more silica is present). To discern changes in the density of the interface, we calculated the average density of the grafted oligomer population, ρ_{graft} , with the assumption of volume additivity

$$\rho_{\text{graft}} = (\rho_{\text{OGN}} - \rho_{\text{NP}}\phi_{\text{NP}})/(1 - \phi_{\text{NP}}) \quad (1)$$

where ρ_{OGN} and $\rho_{\text{NP}} (=2.4 \text{ g mL}^{-1})$ are the respective mass densities of the nanocomposite and the silica nanoparticles, and ϕ_{NP} is the volume fraction of nanoparticles.

The normalized densities $\rho_{\text{NP}}/\rho_{\text{neat}}$ and $\rho_{\text{graft}}/\rho_{\text{neat}}$ in Fig. 2 vary in opposite fashion as a function of silica content. The total mass density reflects the silica concentration, rather than changes in interfacial density. After accounting for the silica content, the oligomer density is seen to decrease with lower grafting density, reflecting the chains pervading a larger local volume. Similar results have been reported previously for polymer nanocomposites with very high silica fractions.²⁶

In Fig. 3 are calorimetry data for the three graft densities, along with that for the neat silica. Note the absence of crystallization for the nanocomposites. While the OGN with the highest grafting density has a distinct glass transition around 226 K , at the lowest σ_g the transition is broadened and shifted

Table 2 Relative silica concentration and density of grafted oligomers

σ_g (nm^{-2})	ρ_{OGN} (g mL^{-1})	SiO_2 (wt%)	ρ_{graft} (g mL^{-1})	$\rho_{\text{graft}}/\rho_{\text{neat}}$
Neat oligomer	1.05 ± 0.01	0	1.05 ± 0.01	1.00
0.59 ± 0.06	1.48 ± 0.01	57	1.03 ± 0.02	0.98 ± 0.03
0.20 ± 0.02	1.67 ± 0.03	72	1.00 ± 0.05	0.96 ± 0.05
0.03 ± 0.003	1.77 ± 0.04	82	0.94 ± 0.06	0.89 ± 0.07

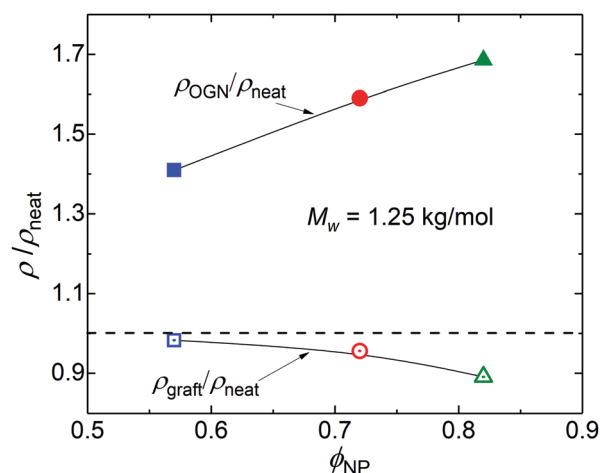


Fig. 2 Ratio of mass densities (ρ_{graft} from eqn (1)) for OGN with varying grafting densities as a function of the relative silica weight fraction. Squares: $\sigma_g = 0.59 \text{ nm}^{-2}$; circles: $\sigma_g = 0.20 \text{ nm}^{-2}$; triangles: $\sigma_g = 0.03 \text{ nm}^{-2}$. Error bars are smaller than the symbol size.

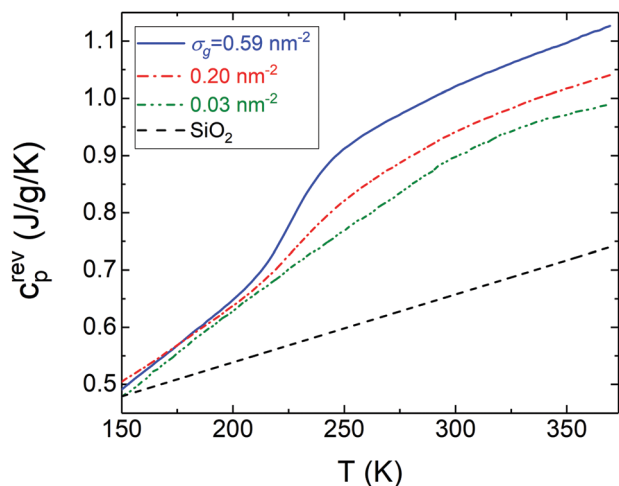


Fig. 3 Reversing heat capacity from TMDSC illustrating the glass transition occurring in the OGN ($M_w = 1.25 \text{ kg mol}^{-1}$).

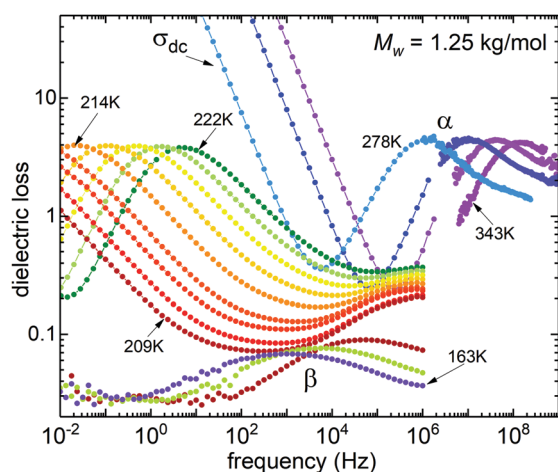


Fig. 4 Representative dielectric loss spectra for the pure oligomer over broad temperature and frequency ranges demonstrating the segmental (α) relaxation and the secondary (β) relaxation, as well as dc-conductivity (σ_{dc}).

by several tens of degrees to higher temperature. More insight into this behavior can be gleaned from dielectric spectroscopy.

Fig. 4 displays the dielectric loss spectra for the neat oligomer ($M_w = 1.25 \text{ kg mol}^{-1}$) measured at various temperatures over a 180 K range. Much of the dynamics are masked by crystallinity; these spectra are omitted (thus, the discontinuity between high and low temperatures). Spectra are shown in Fig. 5 for the corresponding OGN with the highest σ_g ($= 0.59 \text{ nm}^{-2}$); the entire temperature range is accessible because of the absence of crystallization. Three main contributions to the spectra in Fig. 4 and 5 are evident: (1) the segmental relaxation peak at high temperatures; (2) dc-conductivity (σ_{dc}) at intermediate temperatures; and (3) below the glass transition, a secondary (β) relaxation, which has been ascribed to motion of the methylene groups.³⁹ For the OGN, the broad α -peak partially merges with the Maxwell–Wagner–Sillars (MWS) polarization, the latter due to charge buildup at the nanoparticle/oligomer

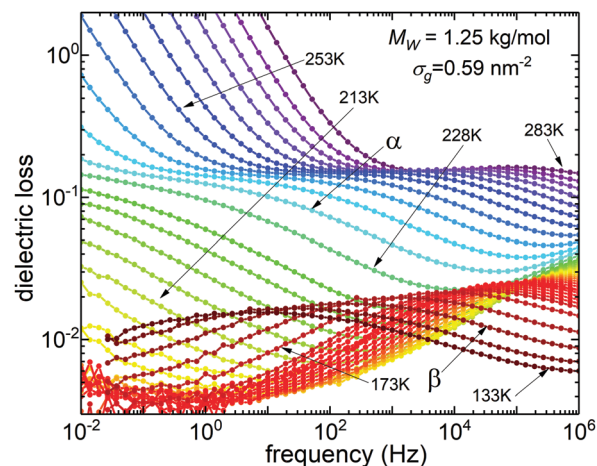


Fig. 5 Dielectric loss spectra of the OGN ($M_w = 1.25 \text{ kg mol}^{-1}$) with the highest grafting density.

interface. The peaks were fit assuming additivity in the frequency domain of the α - and β -relaxations, using for both the Kohlrausch–Williams–Watts (KWW) function⁴⁰

$$\epsilon^*(\omega) = \Delta\epsilon \hat{L} \left(-\frac{d \exp[-(t/\tau)^{\beta_{\text{KWW}}}]}{d\epsilon} \right) + \epsilon_{\infty} \quad (2)$$

with τ , β_{KWW} , and ϵ_{∞} constants, and \hat{L} denotes the Laplace transform. For the MWS contribution, eqn (2) was used with $\beta_{\text{KWW}} = 1$, with a power-law to describe σ_{dc} . The best-fit parameters are listed in Table 3, with the α - and β -relaxation times plotted in Fig. 6 and 7 versus reciprocal temperature and silica concentration respectively. There is a small but systematic decrease in the stretch exponent β_{KWW} as the grafting density is reduced. This reflects broadening of the peak, due to a more heterogeneous local environment. That is, proximity to the particle surface and/or to bonded segments varies because the polymer chain is substantially larger than the interfacial region of the particles.

The data in the supercooled range in Fig. 6 were fit by the Vogel–Fulcher–Tammann–Hesse (VFTH) equation:³⁹

$$\tau_{\alpha} = \tau_0 \exp \left(-\frac{B}{T - T_0} \right) \quad (3)$$

Defining T_g as the temperature at which $\tau_{\alpha} = 10 \text{ s}$, we obtained the values in Table 3. Although T_g is higher for the nanocomposite than for the neat oligomer, the glass transition temperature systematically increases with decrease in the extent of grafting; that is, higher silica concentration. Clearly the

Table 3 Dielectric results for α -process for oligomer with $M_w = 1.25 \text{ kg mol}^{-1}$ and different grafting densities

σ_g	T_g [K] ($\tau_{\alpha} = 10 \text{ s}$)	m	$\beta_{\text{KWW}} (T = T_g)$	E_a^{β} [kJ mol ⁻¹]
Oligomer	212 ± 2	70 ± 5	0.47	42.8 ± 0.4
0.59	226 ± 4	59 ± 6	0.20	42.7 ± 1.0
0.20	234 ± 6	62 ± 7	0.17	36.9 ± 0.6
0.03	246 ± 5	65 ± 5	0.15	36.6 ± 0.8

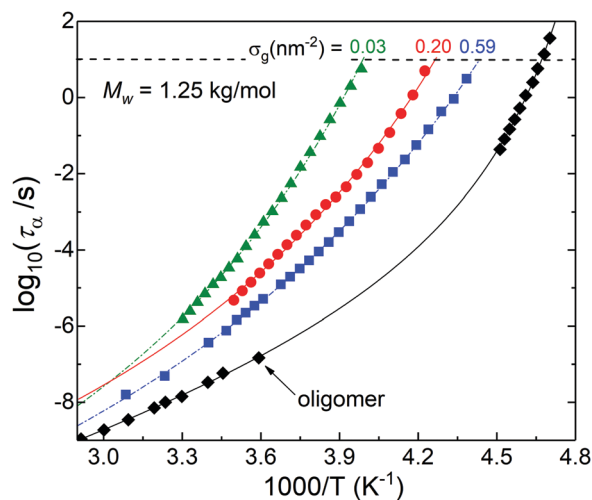


Fig. 6 Arrhenius plot of the segmental relaxation times for the neat oligomer ($M_w = 1.25$ kg mol⁻¹; diamonds) and OGN with different grafting densities (squares: high; circles: intermediate; triangles: low). The gap for the oligomer data is due to crystallization. Lines are VFTH fits (eqn (3)).

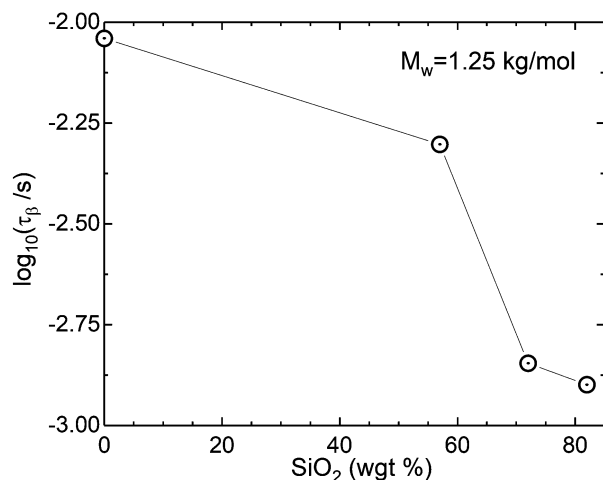


Fig. 7 Relaxation times for the secondary process as a function of silica content (0% = neat oligomer) at $T = 166$ K.

influence of mass density on τ_{α} cannot be isolated from that of grafting density, since pinning of the chains and other interactions with the nanoparticle surface exert a retarding effect on the segmental dynamics. The effect of grafting on the fragility,

$$m = \left. \frac{d \log \tau_{\alpha}}{T_g dT^{-1}} \right|_{T_g},$$

is almost negligible (Table 3).

The effect of grafting on the secondary relaxation is opposite to that on the α process, in that τ_{β} is smaller for the nanocomposite than for the neat oligomer. Moreover, the secondary dynamics become systematically faster with extent of grafting (Fig. 7). The magnitude of the effect is not large (less than an order of magnitude) and saturates at higher temperatures. From the slope of the data below T_g , the activation energy for the β -process can be obtained. There is a small decrease in E_A^{β} when the polymer is grafted to the silica, on the order of 10%,

from the value for the neat oligomer. This change is consistent with the reductions in density, which facilitates the local dynamics. Comparable results were reported by Sokolov and coworkers for both polymer nanocomposites and polymer grafted nanoparticles,^{32,33} as well as Koutsoumpis *et al.* for polymer nanocomposites.³⁶

Effect of molecular weight

Previously it has been found that the molecular weight of the polymer chains (grafted or adsorbed) affects the degree of modification of the dynamics.^{9,26,27} To examine this, we varied the M_w of the poly(tetramethylene oxide) at a constant grafting density, $\sigma_g \approx 0.6$ nm⁻². The mass densities for the OGN were found to be 1.917 ± 0.006 g mL⁻¹ and 1.397 ± 0.001 g mL⁻¹ for the low and high molecular weight samples, respectively. Using eqn (1), this is equivalent to oligomer densities of 1.00 ± 0.01 g mL⁻¹ and 0.996 ± 0.01 g mL⁻¹ respectively. For the shortest chains ($M_w = 0.65$ kg mol⁻¹), the calorimetric glass transition was barely discernable due to the high concentration of silica (82%). For the highest $M_w = 2.25$ kg mol⁻¹ (Fig. 8), there is significant crystallization, but the glass transition temperature can be identified. Both the melting temperature and T_g are essentially unchanged from the values for the neat oligomer. Note that cold crystallization in the vicinity of ambient temperature occurs in the neat oligomer; this is absent for the OGN.

More revealing than calorimetry is dielectric spectroscopy, in which the α - and β -relaxations are clearly evident for all OGN. Fig. 9 shows the temperature dependence of the α -relaxation times for all OGN at constant grafting density (0.6 nm⁻²). For the lowest molecular weight, the α -dynamics becomes as much as 6-orders of magnitude slower, corresponding to about a 58 K increase in T_g . The intermediate molecular weight sample exhibits a weaker effect, 3-orders of magnitude slower α -relaxation (~ 14 K increase in T_g). Over the temperature range for which the highest molecular weight sample can be measured (limited by

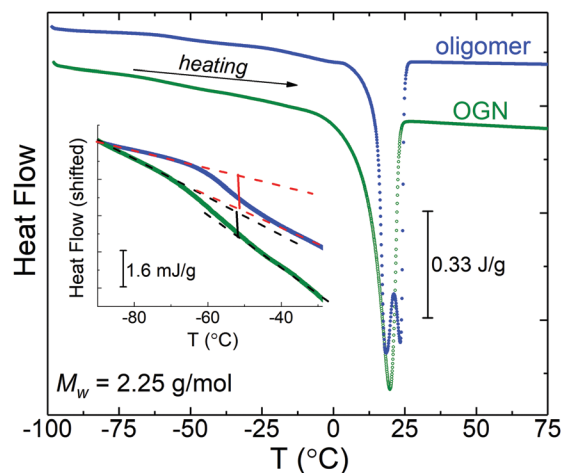


Fig. 8 Differential scanning calorimetry for the high molecular weight oligomer and corresponding OGN at the highest grafting density ($=0.59$ nm⁻²). Inset shows the glass transition region on an expanded scale, with the curves shifted to facilitate comparison.

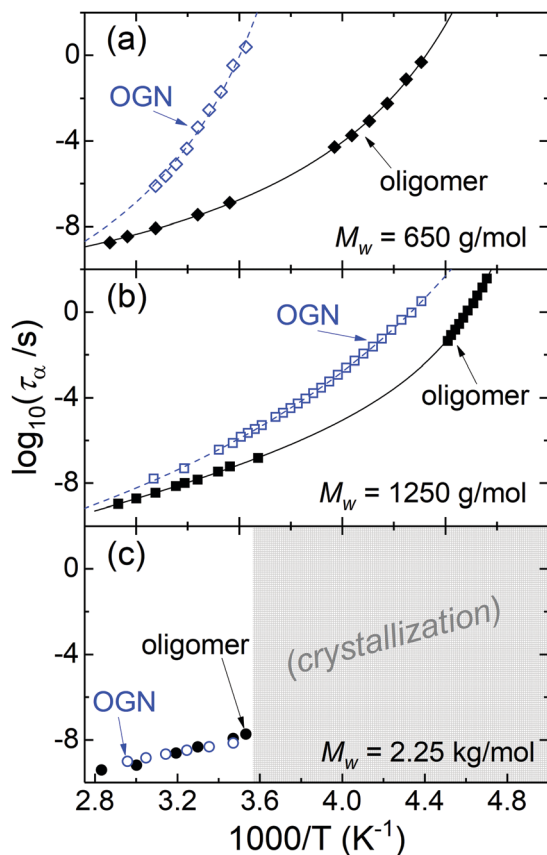


Fig. 9 Temperature dependence of the α -relaxation times for (a) $M_w = 0.65 \text{ kg mol}^{-1}$, (b) $M_w = 1.25 \text{ kg mol}^{-1}$, and (c) $M_w = 2.25 \text{ kg mol}^{-1}$ oligomers (solid symbols) and oligomer grafted nanoparticles (empty symbols) with corresponding VFTH fits (eqn (3)). Error bars are smaller than symbols.

crystallization), no change in relaxation times were observed. This is consistent with the DSC data in Fig. 8.

The temperature dependence of the β -relaxation times in Fig. 10 show a similar trend (albeit opposite – faster dynamics) with M_w of the grafted chains. For the lowest molecular weight, the β -relaxation time decreases by as much as an order of magnitude; this speeding up of the secondary dynamics is less for the intermediate M_w ($=1.25 \text{ kg mol}^{-1}$) OGN. Also, the activation energy (see Table 4) of the lowest molecular weight OGN decreases more so than for the intermediate molecular weight sample, similar to the effect observed with decreasing grafting density seen in Fig. 7. For the highest molecular weight sample, crystallinity precludes definitive conclusions; for this reason we limit the remainder of the discussion to the two non-crystallizing OGN. Note all results for the effect of M_w at constant grafting density are tabulated in Table 4.

Discussion and summary

The effects of grafting density and molecular weight on the dynamics of oligomeric polyamines grafted to silica nanoparticles were investigated. Grafting of the polymer raised its glass transition temperature, although the detailed effects on the

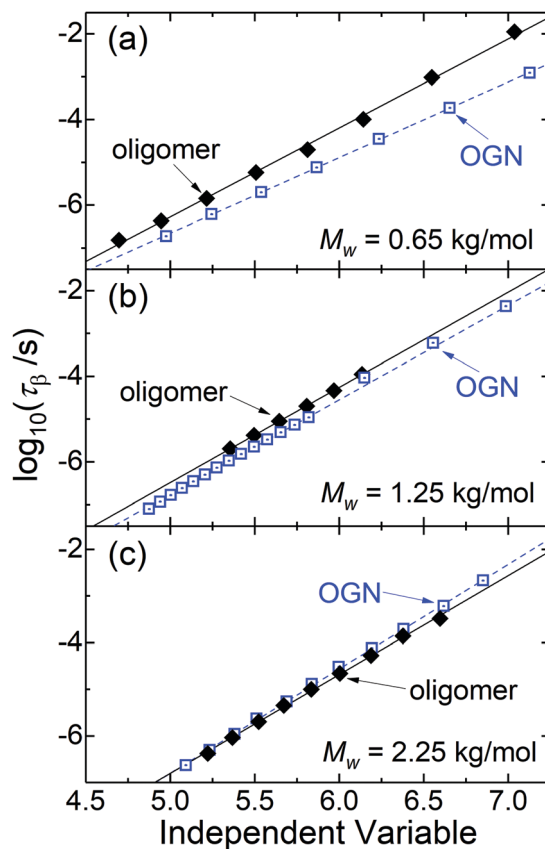


Fig. 10 Temperature dependence of the β -relaxation times for (a) $M_w = 0.65 \text{ kg mol}^{-1}$; (b) 1.25 kg mol^{-1} ; and (c) 2.25 kg mol^{-1} for oligomers (solid symbols) and OGN (open symbols) with corresponding Arrhenius fits. Error bars are smaller than symbol size.

chain dynamics depend both on molecular weight and grafting density. Above T_g the segmental (α) dynamics become slower, but the magnitude of this retardation decreases with increasing graft density and increasing oligomer molecular weight. Slowing of the segmental relaxation for tethered chains is expected, having been demonstrated in many other systems,^{10,11,16–21,27,34,35,41} although there are a few exceptions.^{12,13,42} For the materials having low grafting density, there may be some adsorption of oligomer onto the silica surface, promoted by hydrogen bonding, although the extent of such would be limited by the unfavorable configurations imposed on the chains.

Our finding that the greatest slowing occurs for the lowest M_w oligomer is consistent with recent literature. For example, Kim *et al.*⁹ demonstrated that polyisoprene having $M_w = 3.2 \text{ kg mol}^{-1}$ grafted to silica exhibited segmental relaxation slower by as much as 4 orders of magnitude, while the effect disappeared for molecular weights only twofold higher. For poly(2-vinyl pyridine)/silica nanocomposites, slowing of the segmental dynamics (by about 1.5 orders of magnitude) was greatest for the lowest M_w .²⁷ Similarly, molecular weight dependent slowing of the segmental motions has been shown in polymer nanocomposites with strong polymer-particle attractive interactions, the effect again particularly prominent for low molecular chains.^{26,27,30} Grafting *per se* slows the segmental

Table 4 Results for OGN with equivalent and different molecular weights

M_w (kg mol ⁻¹)	σ_g (nm ⁻²)	SiO ₂ (wt%)	ρ_{graft} (g mL ⁻¹)	T_g ($\tau_\alpha = 10$ s) (K)	m_p	E_A^β (kJ mol ⁻¹)	$\beta_{\text{KWW}} (T = T_g)$
0.65	na	na	1.03	223 ± 2	70 ± 6	39.8 ± 0.7	0.50
0.65	0.60	82	1.00	281 ± 11	70 ± 10	33.8 ± 0.3	0.08
1.25	na	na	1.05	212 ± 2	70 ± 5	42.8 ± 0.4	0.47
1.25	0.60	57	0.98	226 ± 4	59 ± 6	42.7 ± 0.3	0.20
2.25	na	na	1.05	na	na	39.1 ± 0.4	0.49 ^a
2.25	0.58	49	0.99	na	na	42.9 ± 0.3	0.47 ^a

^a Values for the highest molecular weight are for low temperatures prior to crystallization.

dynamics,^{8–11,21,27} analogous to the effect of crosslinking,¹⁴ in which reduced conformational freedom increases τ_α . The consequence of attaching chains to nanoparticles is greater for shorter chains because a higher proportion of segments are in close proximity to the tethered segments and to the confining surface of the particles. This M_w effect has also been shown to occur for physically adsorbed chains in strong hydrogen bonding systems such as poly(2-vinyl pyridine) and silica.⁴³

The speeding up of the β -process observed herein has been reported previously in systems in which the chains were not covalently bound to the nanoparticles.^{12,32,33,36} Molecular dynamics simulations⁴⁴ show that only the α relaxation has strong dynamic correlations; at the β time scale these correlations are weak. This would especially be the case for motion limited to the methylene groups, as herein.³⁸ The implication is that the various factors, including chain stretching^{45–47} and spatial confinement,^{48,49} that influence the segmental dynamics affect the secondary motions more weakly and over a more limited spatial range. Faster β relaxations have been reported for crosslinked polyvinylethylene¹⁴ and glycerol mixed with oligomeric silsesquioxane (POSS),⁵⁰ both materials having increases in density and slower α relaxations. At constant grafting density, we found a significant effect of molecular weight (Table 4) on the activation energies of the β -process for the lowest M_w OGN; however, the effect becomes weaker and even reverses at higher M_w .

The properties changes arising from grafting polymer chains to nanoparticles can potentially be exploited. A possible application is polymer electrolytes, wherein high modulus and high ionic conductivity are desirable. This assumes the ion conduction in polymers below T_g is coupled to the timescale and activation energy of the local secondary relaxations, as has been reported for some polymerized ionic liquids.⁵¹

Conflicts of interest

There are no conflicts to declare.

Acknowledgements

A. P. Holt recognizes the Naval Research Laboratory – American Society of Engineering Education postdoctoral fellowship program. This work was supported by the Office of Naval Research, in part by the Naval Materials Division (R.G. Barsoum, Code 332).

References

- 1 J. Jancar, J. F. Douglas, F. W. Starr, S. K. Kumar, P. Cassagnau, A. J. Lesser, S. S. Sternstein and M. J. Buehler, Current issues in research on structure–property relationships in polymer nanocomposites, *Polymer*, 2010, **51**, 3321–3343.
- 2 D. S. Simmons, An emerging unified view of dynamic interphases in polymers, *Macromol. Chem. Phys.*, 2016, **217**, 137–148.
- 3 F. W. Starr and J. F. Douglas, Modifying fragility and collective motion in polymer melts with nanoparticles, *Phys. Rev. Lett.*, 2011, **106**, 115702.
- 4 P. Z. Hanakata, J. F. Douglas and F. W. Starr, Local variation of fragility and glass transition temperature of ultra-thin supported polymer films, *J. Chem. Phys.*, 2012, **137**, 244901.
- 5 B. A. P. Betancourt, J. F. Douglas and F. W. Starr, Fragility and cooperative motion in a glass-forming polymer–nanoparticle composite, *Soft Matter*, 2013, **9**, 241–254.
- 6 P. Z. Hanakata, J. F. Douglas and F. W. Starr, Interfacial mobility scale determines the scale of collective motion and relaxation rate in polymer films, *Nat. Commun.*, 2014, **5**, 4163.
- 7 S. Choudhury, A. Agrawal, S. A. Kim and L. A. Archer, Self-suspended suspensions of covalently grafted hairy nanoparticles, *Langmuir*, 2015, **31**, 3222–3231.
- 8 A. Agrawal, B. M. Wenning, S. Choudhury and L. A. Archer, Interactions, structure, and dynamics of polymer-tethered nanoparticle blends, *Langmuir*, 2016, **32**, 8698–8708.
- 9 S. A. Kim, R. Mangal and L. A. Archer, Dynamics and rheology of soft colloidal glasses, *Macromolecules*, 2015, **48**, 6280–6293.
- 10 Y. H. Wen, J. L. Schaefer and L. A. Archer, *ACS Macro Lett.*, 2015, **4**, 119–123.
- 11 P. Agarwal, S. A. Kim and L. A. Archer, Crowded, confined, and frustrated: dynamics of molecules tethered to nanoparticles, *Phys. Rev. Lett.*, 2012, **109**, 258301.
- 12 R. Casalini and C. M. Roland, Local and global dynamics in polypropylene glycol/silica composites, *Macromolecules*, 2016, **49**, 3919–3924.
- 13 M. Tyagi, R. Casalini and C. M. Roland, Short time and structural dynamics in polypropylene glycol nanocomposite, *Rubber Chem. Technol.*, 2017, **90**, 264–271.
- 14 R. Casalini and C. M. Roland, Effect of crosslinking on the secondary relaxation in polyvinylethylene, *J. Polym. Sci., Polym. Phys. Ed.*, 2010, **48**, 582–587.

- 15 S. K. Kumar and R. Krishnamoorti, Nanocomposites: structure, phase behavior, and properties, *Annu. Rev. Chem. Biomol. Eng.*, 2010, **1**, 37–58.
- 16 A. Bansal, H. Yang, C. Li, K. Cho, B. C. Benicewicz, S. K. Kumar and L. S. Schadler, Quantitative equivalence between polymer nanocomposites and thin polymer films, *Nat. Mater.*, 2005, **4**, 693–698.
- 17 A. P. Holt, J. R. Sangoro, Y. Wang, A. L. Agapov and A. P. Sokolov, Chain and segmental dynamics of poly(2-vinylpyridine) nanocomposites, *Macromolecules*, 2013, **46**, 4168–4173.
- 18 J. Moll and S. K. Kumar, Segmental dynamics of polymer melts with spherical nanoparticles, *Macromolecules*, 2012, **45**, 1131–1135.
- 19 A. P. Holt, P. J. Griffin, V. Bocharova, A. L. Agapov, A. E. Imel, M. D. Dadmun, J. R. Sangoro and A. P. Sokolov, *Macromolecules*, 2014, **47**, 1837–1843.
- 20 S. Gong, Q. Chen, J. F. Moll, S. K. Kumar and R. H. Colby, *ACS Macro Lett.*, 2014, **3**, 773–777.
- 21 C. G. Robertson and C. M. Roland, Glass transition and interfacial segmental dynamics in polymer-particle composites, *Rubber Chem. Technol.*, 2008, **81**, 506–522.
- 22 C. J. T. Landry and P. M. Henrichs, The influence of blending on the local motions of polymers. Studies involving polycarbonate, poly(methyl methacrylate), and a polyester, *Macromolecules*, 1989, **22**, 2157–2166.
- 23 K. L. Ngai, R. W. Rendell and A. F. Yee, Local molecular motions in glassy and dissolved polycarbonates, *Macromolecules*, 1988, **21**, 3396–3401.
- 24 C. Xiao, J. Y. Jho and A. F. Yee, Correlation between the shear yielding behavior and secondary relaxations of bisphenol a polycarbonate and related copolymers, *Macromolecules*, 1994, **27**, 2761–2768.
- 25 R. Casalini and C. M. Roland, Anomalous properties of the local dynamics in polymer glasses, *J. Chem. Phys.*, 2009, **131**, 1–6.
- 26 S. Cheng, A. P. Holt, H. Wang, F. Fan, V. Bocharova, H. Martin, T. Etampawala, B. T. White, T. Saito, N. G. Kang, M. D. Dadmun, J. W. Mays and A. P. Sokolov, Unexpected molecular weight effect in polymer nanocomposites, *Phys. Rev. Lett.*, 2016, **116**, 038302.
- 27 A. P. Holt, V. Bocharova, S. Cheng, A. M. Kisliuk, B. T. White, T. Saito, D. Uhrig, J. P. Mahalik, R. Kumar, A. E. Imel, T. Etampawala, H. Martin, N. Sikes, B. G. Sumpter, M. D. Dadmun and A. P. Sokolov, Controlling interfacial dynamics: covalent bonding versus physical adsorption in polymer nanocomposites, *ACS Nano*, 2016, **10**, 6843–6852.
- 28 S. Cheng, B. Carroll, W. Lu, F. Fan, J. M. Carrillo, H. Martin, A. P. Holt, N. G. Kang, V. Bocharova, J. W. Mays, B. G. Sumpter, M. D. Dadmun and A. P. Sokolov, Interfacial properties of polymer nanocomposites: Role of chain rigidity and dynamic heterogeneity length scale, *Macromolecules*, 2017, **50**, 2397–2406.
- 29 S. Cheng, B. Carroll, V. Bocharova, J. M. Carrillo, B. G. Sumpter and A. P. Sokolov, Focus: Structure and dynamics of the interfacial layer in polymer nanocomposites with attractive interactions, *J. Chem. Phys.*, 2017, **146**, 203201.
- 30 P. Klonos, K. Kulyk, M. V. Borysenko, V. M. Gun'ko, A. Kyritsis and P. Pissis, Effects of molecular weight below the entanglement threshold on interfacial nanoparticles/polymer dynamics, *Macromolecules*, 2016, **49**, 9457–9473.
- 31 S. Y. Kim, H. W. Meyer, K. Saalwächter and C. F. Zukoski, Polymer dynamics in PEG-Silica nanocomposites: Effects of polymer molecular weight, temperature and solvent dilution, *Macromolecules*, 2012, **45**, 4225–4237.
- 32 Y. Ding, S. Pawlus, A. P. Sokolov, J. F. Douglas, A. Karim and C. L. Soles, Dielectric Spectroscopy Investigation of Relaxation in C₆₀-Polyisoprene Nanocomposites, *Macromolecules*, 2009, **42**, 3201–3206.
- 33 A. P. Holt, V. Bocharova, S. Cheng, A. M. Kisliuk, G. Ehlers, E. Mamontov, V. N. Novikov and A. P. Sokolov, Interplay between local dynamics and mechanical reinforcement in glassy polymer nanocomposites, *Phys. Rev. Mater.*, 2017, **1**, 062601.
- 34 J. H. Roh, M. Tyagi, T. E. Hogan and C. M. Roland, Space-dependent dynamics in 1,4-polybutadiene nanocomposite, *Macromolecules*, 2013, **46**, 6667–6669.
- 35 J. H. Roh, M. Tyagi, T. E. Hogan and C. M. Roland, Effect of binding to carbon black on the dynamics of 1,4-polybutadiene, *J. Chem. Phys.*, 2013, **139**, 134905.
- 36 S. Koutsoumpis, A. Poulakis, P. Klonos, S. Kriptou, V. Tsanakis, D. N. Bikiaris, A. Kyritsis and P. Pissis, Structure, thermal transitions and polymer dynamics in nanocomposites based on poly(ϵ -caprolactone) and nano-inclusions of 1-3D geometry, *Thermochim. Acta*, 2018, **666**, 229–240.
- 37 J. A. Miller, G. Pruckmayr, E. Epperson and S. L. Cooper, The thermal response of the polyether soft segment chain conformation in a polyurethane block copolymer measured by small-angle neutron scattering, *Polymer*, 1985, **26**, 1915–1920.
- 38 F. Fug, K. Rohe, J. V. Vargas, C. Nies, M. Springborg and W. Possart, 4,4'-Methylene diphenyl diisocyanate – conformational space, normal vibrations and infrared spectra, *Polymer*, 2016, **99**, 671–683.
- 39 H. N. Ng, A. E. Allegranza, R. W. Seymour and S. L. Cooper, Effect of segment size and polydispersity on properties of polyurethane block polymers, *Polymer*, 1973, **14**, 255–261.
- 40 C. M. Roland, *Viscoelastic Behavior of Rubbery Materials*, Oxford University Press, 2011.
- 41 R. Casalini, R. Bogoslovov, S. B. Qadri and C. M. Roland, Nanofiller reinforcement of elastomeric polyurea, *Polymer*, 2012, **53**, 1282–1287.
- 42 R. B. Bogoslovov, C. M. Roland, A. R. Ellis, A. M. Randall and C. G. Robertson, Effect of silica nanoparticles on the local segmental dynamics in poly(vinyl acetate), *Macromolecules*, 2008, **41**, 1289–1296.
- 43 D. N. Voylov, A. P. Holt, B. Doughty, V. Bocharova, H. M. Meyer, S. Cheng, H. Martin, M. Dadmun, A. Kisliuk and A. P. Sokolov, Unraveling the molecular weight dependence of interfacial interactions in poly(2-vinyl pyridine)/silica nanocomposites, *ACS Macro Lett.*, 2017, **6**(2), 68–72.
- 44 D. Fragiadakis and C. M. Roland, Dynamic correlations and heterogeneity in the primary and secondary relaxations of a

- model molecular liquid, *Phys. Rev. E: Stat., Nonlinear, Soft Matter Phys.*, 2014, **89**, 052304.
- 45 F. T. Oyerokun and K. S. Schweizer, Theory of glassy dynamics in conformationally anisotropic polymer systems, *J. Chem. Phys.*, 2005, **123**, 224901.
- 46 J. Khouri and G. P. Johari, Note: effects of adding a viscosity-increasing 2 nm-size molecule on dielectric relaxation features and the dynamic heterogeneity view, *J. Chem. Phys.*, 2013, **138**, 196101.
- 47 H. Lee, J. Pietrasik, S. S. Sheiko and K. Matyjaszewski, Stimuli-responsive molecular brushes, *Prog. Polym. Sci.*, 2010, **35**, 24–44.
- 48 R. Richert, Dynamics of nanoconfined supercooled liquids, *Annu. Rev. Phys. Chem.*, 2011, **62**, 65–84.
- 49 M. Alcoutlabi and G. B. McKenna, Effects of confinement on material behaviour at the nanometre size scale, *J. Phys.: Condens. Matter*, 2005, **17**, R461.
- 50 S. Gupta, J. K. H. Fischer, P. Lunkenheimer, A. Loidl, E. Novak, N. Jalarvo and M. Ohl, Effect of adding nanometre-sized heterogeneities on the structural dynamics and the excess wing of a molecular glass former, *Sci. Rep.*, 2016, **6**, 35034.
- 51 Z. Wojnarowska, F. Hongbo, Y. Fu, S. Cheng, B. Carroll, R. Kumar, V. N. Novikov, A. M. Kisliuk, T. Saito, N. G. Kang, J. W. Mays, A. P. Sokolov and V. B. Bocharova, Effect of chain rigidity on the decoupling of ion motion from segmental relaxation in polymerized ionic liquids: ambient and elevated pressure studies, *Macromolecules*, 2017, **50**, 6710–6721.